



# A Critical Role for $\gamma$ CaMKII in Decoding NMDA Signaling to Regulate AMPA Receptors in Putative Inhibitory Interneurons

Xingzhi He<sup>1,2</sup> · Yang Wang<sup>1,2</sup> · Guangjun Zhou<sup>1,2</sup> · Jing Yang<sup>1,2</sup> · Jiarui Li<sup>1,2</sup> · Tao Li<sup>1,2</sup> · Hailan Hu<sup>1,2,3</sup> · Huan Ma<sup>1,2,3</sup>

Received: 13 September 2021 / Accepted: 20 December 2021 / Published online: 15 March 2022  
© Center for Excellence in Brain Science and Intelligence Technology, Chinese Academy of Sciences 2022

**Abstract** CaMKII is essential for long-term potentiation (LTP), a process in which synaptic strength is increased following the acquisition of information. Among the four CaMKII isoforms,  $\gamma$ CaMKII is the one that mediates the LTP of excitatory synapses onto inhibitory interneurons (LTP<sub>E→I</sub>). However, the molecular mechanism underlying how  $\gamma$ CaMKII mediates LTP<sub>E→I</sub> remains unclear. Here, we show that  $\gamma$ CaMKII is highly enriched in cultured hippocampal inhibitory interneurons and opts to be activated by higher stimulating frequencies in the 10–30 Hz range. Following stimulation,  $\gamma$ CaMKII is translocated to the synapse and becomes co-localized with the postsynaptic protein PSD-95. Knocking down  $\gamma$ CaMKII prevents the chemical LTP-induced phosphorylation and trafficking of AMPA receptors (AMPA) in putative inhibitory interneurons, which are restored by overexpression of  $\gamma$ CaMKII but not its kinase-dead form. Taken together, these data suggest that  $\gamma$ CaMKII decodes NMDAR-mediated signaling and in turn regulates AMPARs for expressing LTP in inhibitory interneurons.

**Keywords** Synaptic plasticity · LTP · Inhibitory interneurons ·  $\gamma$ CaMKII · AMPAR · NMDAR

## Introduction

Mapping the cellular and molecular substrates of long-term synaptic plasticity has been a fundamental goal of neuroscience, with significant implications for neurotherapeutics and nootropics. A major form of long-term synaptic plasticity, long-term potentiation (LTP) allows neurons to change their synaptic strength following the acquisition of information [1]. Since its initial discovery, extensive studies involving the LTP of excitatory synapses onto excitatory neurons (LTP<sub>E→E</sub>) have advanced our understanding of its underlying molecular mechanisms and functional roles, leading to a widely accepted cellular model of learning and memory [2–5]. By coordinating with excitatory neurons, the plasticity of inhibitory interneurons is essential for dynamic control of the overall level of excitatory activity and information process in the brain. However, unlike LTP<sub>E→E</sub>, the molecular mechanisms that underlie the LTP of excitatory synapses onto inhibitory interneurons (LTP<sub>E→I</sub>) [6–9] remain largely unknown.

In the canonical LTP<sub>E→E</sub> induction pathway, the activation of N-methyl-D-aspartate receptors (NMDARs) [10] is critical for triggering signal transduction and in turn regulates  $\alpha$ -amino-3-hydroxy-5-methyl-4-isoxazolepropionic acid receptor (AMPA) function [2, 3]. In this fundamental process,  $\alpha$ CaMKII ( $\alpha$  Ca<sup>2+</sup>/calmodulin-dependent protein kinase II) serves as the central regulator by decoding NMDAR signaling to control AMPAR phosphorylation and membrane trafficking [11–13]. Similar to excitatory neurons, NMDARs and AMPARs are also present and are known to play a critical role in regulating

Xingzhi He and Yang Wang have contributed equally to this work.

✉ Huan Ma  
mah@zju.edu.cn

<sup>1</sup> Department of Neurobiology, Affiliated Mental Health Center and Hangzhou Seventh People's Hospital, Zhejiang University School of Medicine, Hangzhou 310058, China

<sup>2</sup> NHC and CAMS Key Laboratory of Medical Neurobiology, MOE Frontier Science Center for Brain Research and Brain-Machine Integration, School of Brain Science and Brain Medicine, Zhejiang University, Hangzhou 310058, China

<sup>3</sup> Research Units for Emotion and Emotion disorders, Chinese Academy of Medical Sciences, Beijing 100730, China

postsynaptic  $\text{Ca}^{2+}$  signaling and controlling excitatory input in inhibitory interneurons [5, 14–16]. Although  $\alpha$ CaMKII is not expressed in inhibitory neurons [17],  $\gamma$ CaMKII is robustly expressed in inhibitory interneurons and is a mediator of  $\text{LTP}_{\text{E} \rightarrow \text{I}}$  in the hippocampus [18]. However, the molecular mechanisms underlying the role of  $\gamma$ CaMKII in  $\text{LTP}_{\text{E} \rightarrow \text{I}}$  remain unclear. A limitation of the previous work [18] is that the functional role of  $\gamma$ CaMKII in mediating NMDAR-triggered AMPAR trafficking was not directly examined. This is important as  $\text{Ca}^{2+}$ -permeable AMPARs are known to be strongly expressed in inhibitory interneurons and the expression of NMDARs is relatively low [16, 19], which raises the question of whether  $\gamma$ CaMKII mediates  $\text{LTP}_{\text{E} \rightarrow \text{I}}$  by regulating AMPAR function in an NMDAR-dependent manner. Here, we studied the role of  $\gamma$ CaMKII in this process using a glycine-based chemical LTP (cLTP) paradigm in cultured hippocampal neurons. Applying this approach provided two key advantages over the simple electrophysiological assays used in the previous study [18]. First, using this system minimized compensatory effects that might take place during the development period because of the absence of  $\gamma$ CaMKII. Further, we easily monitored the subcellular localization of  $\gamma$ CaMKII and AMPARs at relatively high resolution in cultured neurons to assess the expression of surface AMPARs.

By combining cellular studies with immuno-electron microscopy and electrophysiological analysis, we found that cultured  $\alpha$ CaMKII-negative neurons (i.e., inhibitory interneurons) expressed CaMKII phosphorylated at Thr-286/287 (pCaMKII). Compared to  $\alpha$ CaMKII-positive neurons (i.e., excitatory interneurons), pCaMKII in putative inhibitory ( $\alpha$ CaMKII-negative) neurons were recruited by field stimuli at relatively high frequencies (10–30 Hz). Knocking down  $\gamma$ CaMKII using specific small hairpin RNA (shRNA) eliminated pCaMKII in these cells, suggesting that  $\gamma$ CaMKII is the main isoform of functional CaMKII.  $\gamma$ CaMKII exerted activity-dependent translocation to co-localize with the postsynaptic protein PSD-95 following cLTP stimulation. Knocking down  $\gamma$ CaMKII prevented the phosphorylation of the AMPAR subunit GluA1 at Ser831 (pGluA1) and inhibited the NMDAR-dependent changes of surface GluA1 level, which were rescued by an shRNA-resistant  $\gamma$ CaMKII, but not the kinase-dead form of  $\gamma$ CaMKII. Taken together, these results suggest that  $\gamma$ CaMKII mediates  $\text{LTP}_{\text{E} \rightarrow \text{I}}$  by decoding postsynaptic NMDAR signaling and in turn regulating AMPAR function.

## Materials and Methods

### Data Acquisition

All data were acquired and analyzed by experimenters who were blinded with respect to the cultured neurons and stimulating conditions.

### Animals

C57BL/6J mice and Sprague-Dawley rats were purchased from Shanghai SLAC Laboratory Animal Co., Ltd. All animal studies and experimental procedures were approved by the Animal Care and Use Committee at Zhejiang University.

### Primary Cultures of Hippocampal Neurons

Hippocampal neurons were cultured from Sprague-Dawley rat pups at postnatal days 0–1. The hippocampus was isolated and washed twice in ice-cold modified Hanks' balanced salt solution (HBSS; 4.2 mmol/L  $\text{NaHCO}_3$  and 1 mmol/L HEPES, pH 7.35, 300 mOsm) containing 20% fetal bovine serum (FBS; Hyclone, Logan, USA). The tissue was digested for 30 min in 2.5 mL FBS-free HBSS containing 145 U papain (Worthington Biochemical Corp., Lakewood, USA) and 40  $\mu\text{L}$  DNase at 37 °C with gentle shaking every 10 min. Digestion was stopped by adding 5 mL modified HBSS containing 20% FBS. After washing, the digested tissue was dissociated using Pasteur pipettes of decreasing diameter. The resulting cell suspensions were pelleted twice, filtered through a 70- $\mu\text{m}$  nylon strainer, and then plated on 12-mm round coverslips coated with poly-D-lysine. The cultures were maintained in NbActiv4 medium (BrainBits, Springfield, USA). Every 7 days, 30% of the medium was replaced with fresh medium. The neurons were processed for further experiments 10–17 days after plating.

### Plasmid Generation

The rat  $\gamma$ CaMKII shRNA sequence (5'-TGGCCTGGCCA TCGAAGTGCA-3') was subcloned into the pLVTHM vector (12247, Addgene, Watertown, USA) following the manufacturers' protocol [20]. Plasmids of pAAV-hSyn-mCherry-P2A-HA-Hs $\gamma$ CaMKII (WT) and pAAV-hSyn-mCherry-P2A-HA-Hs $\gamma$ CaMKII (K43R) were generated as described previously [18]. In brief, the pAAV-hSyn-mCherry-P2A-HA-Hs $\gamma$ CaMKII (WT) plasmid was assembled by homologous recombination of a linearized pAAV backbone (114472, Addgene), P2A was amplified from pC5Kan-P2A (51814, Addgene), and HA-Hs $\gamma$ CaMKII

(WT) was amplified from pCDH-EF1 $\alpha$ -HA-Hs $\gamma$ CaMKII (WT) [21]. The pAAV-hSyn-mCherry-P2A-HA-Hs $\gamma$ CaMKII (K43R) plasmid was generated using PCR-based mutagenesis.

### Field Stimulation

Field stimuli were applied as previously described [20]. In brief, we applied 3-ms square-wave pulses to stimulate cultured hippocampal neurons using two platinum electrodes spaced  $\sim$ 10 mm apart. We used the stimulator (Grass S11; Grass Instruments, Quincy, USA) to control the pulse amplitude and duration. To achieve a reliable effect, we set the stimulating amplitude 20% above the threshold.

### Neuronal Stimulation and Immunocytochemistry

To stimulate neurons, we added 30  $\mu$ mol/L NMDA (M3262; Sigma, St. Louis, USA) to cultures of hippocampal neurons at room temperature for 60 s. To induce chemical LTP, cultured hippocampal neurons were treated with 200  $\mu$ mol/L glycine (G5417; Sigma) in an extracellular solution containing 5 mmol/L KCl, 143 mmol/L NaCl, 10 mmol/L HEPES, 10 mmol/L glucose, 2 mmol/L CaCl<sub>2</sub>, 0.5  $\mu$ mol/L TTX (abs44200985a; Absin, Shanghai, China), 1  $\mu$ mol/L strychnine (45661; Sigma), and 20  $\mu$ mol/L bicuculline (HY-N0219; MedChemExpress, Monmouth Junction, USA) for 10 min at room temperature. The stimulated neurons were fixed at different time points following the stimulation in fixing solution containing 4% (v/v) paraformaldehyde, 4% (w/v) sucrose, and 20 mmol/L EGTA in PBS buffer for 15 min. The fixed cells were permeabilized with 0.1% Triton X-100 and blocked with 7.5% normal donkey serum before incubation with primary antibodies overnight at 4°C. The primary antibodies were as follows: rabbit anti- $\gamma$ CaMKII (1:2000) raised against amino-acids 441–458 (we refer to this antibody as ab01; GL Biochem; Shanghai, China [18]); mouse anti- $\alpha$ CaMKII (1:1000, MA1-048; Thermo Fisher Scientific, Waltham, USA); mouse anti-PSD95 (1:1000, 36233S; Cell Signaling Technology, Danvers, USA); rabbit anti-pCaMKII (1:2000, 12716, Cell Signaling Technology); or rabbit anti-pGluA1 (1:1000, AB5847; Millipore, Billerica, USA). The cells were then washed for 10 min in PBS, followed by incubation with secondary antibodies (1:2000, A21202, A21206, A31570-31573; Invitrogen, Carlsbad, USA) at room temperature for 1 h. A Nikon A1 confocal microscope system (Nikon, Tokyo, Japan) using either a 40 $\times$  or a 60 $\times$  objective was used to acquire fixed neuron images.

For labeling of surface GluA1, the neurons were labeled with an antibody against mouse N-terminal GluA1 (1:500, MAB2263, Millipore). After incubation for 30 min at

37°C, the cells were immediately fixed in fixing solution for 10 min. Surface antibody-labeled GluA1 was saturated with anti-mouse Alexa-Fluor 647 (1:2000, A31571, Invitrogen/Life Technologies) for 40 min, followed by washing with PBS for 30 min.

### Electron Microscopy

Under deep anesthesia, mice were perfused with 0.9% saline, followed by 0.1% glutaraldehyde and 4% paraformaldehyde dissolved in 0.1 mol/L phosphate buffer. The whole brain was removed and post-fixed overnight in 4% paraformaldehyde and 0.1% glutaraldehyde in 0.1 mol/L phosphate buffer. Brain sections (50  $\mu$ m thick) were cut on a vibratome (Microm HM 430; ThermoFisher Scientific). Sections containing the hippocampus were collected and incubated in 50 mmol/L glycine for 30 min. The sections were permeabilized with 0.05% Triton X-100 in phosphate buffer for 15 min and then blocked with blocking buffer consisting of 0.1% BSA-C<sup>TM</sup> (Aurion; Immuno Gold Reagents & Accessories, Wageningen, Netherlands) in 0.1 mol/L PBS for 30 min. After washing twice with blocking buffer, the sections were incubated with rabbit anti- $\gamma$ CaMKII antibody (1:500, ab01) in blocking buffer at 4°C for  $\sim$ 12 h. After washing 6 times with washing buffer (10 min each), the sections were incubated overnight with Nano gold-labeled Fab' anti-rabbit secondary antibody in blocking buffer at 4°C. After washing 6 times (10 min each), followed by 2 washes with PBS (10 min each), the sections were fixed with 2.5% glutaraldehyde in PBS for 2 h, washed 3 times with PBS (10 min each), washed 6 times with deionized water (10 min each), and washed 3 times with 0.02 mol/L sodium citrate buffer (pH 7.0) (5 min each). The sections were treated for 6–8 min using an HQ Silver Enhancement Kit (Nanoprobes Inc., Yaphank, USA), followed by 6 washes with deionized water (10 min each) and 3 washes with 0.1 mol/L PBS (5 min each). The sections were then treated with 1% OsO<sub>4</sub> in 0.1 mol/L PBS for 30 min, followed by staining with 2% uranyl acetate for 30 min. The sections were then dehydrated in gradient ethanol and 100% acetone, and then embedded in EPON resin. After the resin polymerized, the sections were cut into 70-nm ultrathin sections using a diamond knife mounted on an ultramicrotome. The ultrathin sections were then mounted on single-slot grids coated with a pioloform membrane, stained with 1% (w/v) lead citrate, and examined using an electron microscope (Philips Tecnai 20 transmission electron microscope at the Center for Cryo-Electron Microscopy, Zhejiang University, Hangzhou, China). Typical synaptic structures were imaged.

## RNA Extraction and cDNA Reverse Transcription

Total RNA was extracted from hippocampal cultured cells using TRIzol (93289; Sigma-Aldrich) based on the manufacturer's instructions. Briefly, cells were rapidly homogenized in the TRIzol reagent. Chloroform was added to the supernatant, then vortexed and centrifuged at 4 °C for 15 min. Isopropyl alcohol was added to the aqueous phase. The samples were vortexed and incubated at room temperature for 10 min followed by centrifugation at 4 °C for 10 min. The precipitates were washed twice in 75% ethanol and centrifuged at 4 °C for 5 min. Total RNA was reverse-transcribed into cDNA using the Goldenstar RT6 cDNA Synthesis Kit Ver. 2 (TSK302M; TsingKe, Shanghai, China) based on the manufacturer's instructions and used immediately or stored at  $-20$  °C.

## Quantitative Real-Time PCR

PCR amplification of cDNA was applied using the Hieff qPCR SYBR Green Master Mix (11201ES08; Yeasen Biotechnology, Shanghai, China) in 96-well plates (Bio-Rad, Hercules, USA). Relative gene expression in mRNA levels was quantified using the  $2^{-\Delta\Delta C_t}$  method. The mean  $C_t$  of *GAPDH* (internal control gene) was subtracted from the mean  $C_t$  of each target gene ( $\Delta C_t$ ). Fold change was calculated by normalizing each  $\Delta\Delta C_t$  value to the corresponding control  $\Delta\Delta C_t$  value. For each experimental sample, triplicate reactions were conducted using the following qRT-PCR primers: Fwd: 5'-AACCTGCCAAGTATGATGACATCA-3' and Rev: 5'-TGTTGAAGTCA-CAGGAGACAACCT-3' for *GAPDH*; Fwd: 5'-AAGAAGTTGTCTGCCCGAGA-3' and Rev: 5'-CCTCCCGTAACA AGGTCAAA-3' for *CaMK2G*.

## Statistical Analysis

Data were analyzed using GraphPad Prism (GraphPad Software, San Diego, USA), and the statistical analysis was performed using one-way ANOVA followed by Tukey's test or unpaired Student's *t*-test. We considered a *P*-value  $<0.05$  as statistically significant.

## Results

### CaMKII in Putative Inhibitory Interneurons is Preferentially Activated by High-Frequency Stimuli

By virtue of its autonomous kinase activity through the phosphorylation of Thr-286/287 in its regulatory domain, CaMKII is well suited for decoding  $Ca^{2+}$  signals and regulating synaptic plasticity [12, 22]. CaMKII comprises a

family of isoforms ( $\alpha$ ,  $\beta$ ,  $\gamma$ , and  $\delta$ ) derived from four closely-related yet distinct genes (*CaMK2A*, *CaMK2B*, *CaMK2G*, and *CaMK2D*), which are highly enriched in brain tissue and present throughout the body. As a classic marker for excitatory neurons such as glutamatergic principal neurons [17], the expression of  $\alpha$ CaMKII in the brain is highly cell-specific and most  $\alpha$ CaMKII-negative cells are thought to be inhibitory interneurons [21]. Autophosphorylation of CaMKII at Thr-286/287 (pCaMKII) enables CaMKII to decode the graded translation of  $Ca^{2+}$  spike frequency into kinase activity *in vitro* [23] and in intact neurons [24], which can be monitored by using a specific pCaMKII antibody that recognizes all phosphorylated CaMKII isoforms [20, 25].

Inspired by the finding that  $Ca^{2+}/CaM$  and CaMKII signaling cascades are critical for  $LTP_{E\rightarrow I}$  [18, 26, 27], we first examined the activation patterns of CaMKII in cultured hippocampal neurons. To mimic neuronal activity under physiological conditions, we applied field electric stimulation to evoke trains of action potentials over a wide range of frequencies [28], which were prevented by applying  $Na^+$  channel blockade—tetrodotoxin (TTX). Cultured neurons were able to generate spikes at frequencies as high as 50 Hz, which are illustrated by representative traces of current-clamp recordings of membrane potential (Fig. 1A). Measurements of dendritic pCaMKII responses showed a striking dependence on stimulus frequency and the cell type (Fig. 1B, C). In putative excitatory neurons ( $\alpha$ CaMKII-positive neurons), 5-Hz stimulation was the most effective frequency for inducing CaMKII phosphorylation, significantly more so than lower or higher test frequencies (Fig. 1B, C). In contrast, pCaMKII was only induced by higher frequencies such as 10 Hz and 30 Hz (Fig. 1B, C) in putative inhibitory interneurons ( $\alpha$ CaMKII-negative neurons). Given that different CaMKII isoforms have distinct phosphorylation rates [29], these results indicate that the CaMKII isoforms expressed in inhibitory interneurons are different from those in excitatory neurons.

### $\gamma$ CaMKII is the Predominant CaMKII Isoform that Functions in Putative Interneurons

The field electric stimulation provides a convenient way of activating neurons in a relatively physiological manner, creating a simple platform for quantitative analysis of the activity-dependent CaMKII phosphorylation in cultured neurons. Having characterized the basic features of CaMKII activation in this way, we next sought the functional isoform of CaMKII that is responsible for the frequency-dependent CaMKII activation recorded in inhibitory interneurons. Among different CaMKII isoforms,  $\gamma$ CaMKII appears to be a logical candidate, as  $\gamma$ CaMKII

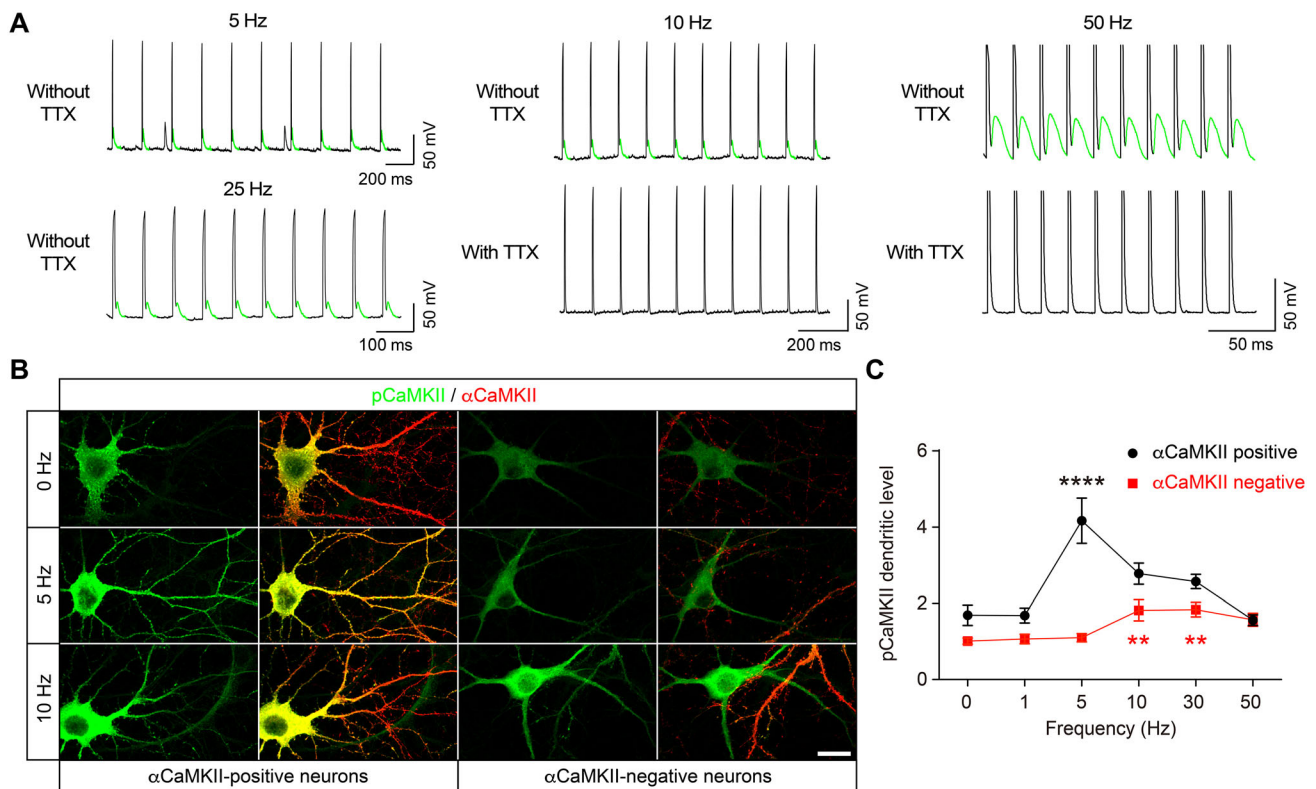


**Fig. 1** Activation pattern of CaMKII in excitatory neurons and putative inhibitory interneurons. **A** Representative traces recorded using current clamp in cultured hippocampal neurons that are stimulated in the presence or absence of 0.5  $\mu\text{mol/L}$  TTX. Neuronal spikes are activated by field stimulation at various frequencies, achieving firing frequencies as high as 50 Hz. **B, C** Representative images (**B**) and analysis (**C**) of CaMKII activation (pCaMKII) in  $\alpha\text{CaMKII}$ -positive (excitatory neurons) and  $\alpha\text{CaMKII}$ -negative (putative interneurons) neurons after field stimulation at different

frequencies. Data are normalized to the 0 Hz control ( $n = 19\text{--}41$  cells from two independent cultures). In this and subsequent figures, data are normalized to the unstimulated control, and are presented as the mean  $\pm$  SEM.  $**P < 0.01$  (10 Hz or 30 Hz vs 0 Hz stimulation) and  $****P < 0.0001$  (5 Hz vs 0 Hz stimulation), unpaired Student's  $t$ -test. Scale bar, 20  $\mu\text{m}$ . In this and subsequent results, neurons with low or no  $\alpha\text{CaMKII}$  expression and very few spines are defined as putative interneurons [31].

has the slowest autophosphorylation rate among the isoforms [29]. Indeed, this feature of  $\gamma\text{CaMKII}$  might be functionally important because it allows  $\gamma\text{CaMKII}$  to decode larger and longer  $\text{Ca}^{2+}$  signals induced in inhibitory interneurons, which normally fire at a high frequency [23, 30, 31].

To address whether  $\gamma\text{CaMKII}$  is responsible for the pCaMKII dynamics and functions recorded in inhibitory interneurons, we induced LTP in cultured neurons using a classic cLTP protocol [32], which reliably increases surface AMPARs [28]. As expected, cLTP activated CaMKII and induced pCaMKII in both excitatory and putative inhibitory interneurons (Fig. 2A). To test for a causal role of  $\gamma\text{CaMKII}$  in this process, we knocked down  $\gamma\text{CaMKII}$  using lentiviral-mediated transfer of short-hairpin RNAs (shRNAs). The mRNA level of  $\gamma\text{CaMKII}$  was reduced by  $\sim 75\%$ , relative to cells infected with a control lentivirus expressing non-silencing shRNA (Fig. 2B). Importantly, we found that the activation of CaMKII in putative interneurons induced by cLTP was prevented by

knocking down  $\gamma\text{CaMKII}$  using shRNA [20, 21] (Fig. 2C, D), suggesting that  $\gamma\text{CaMKII}$  is the predominant CaMKII subunit that plays a critical role in putative inhibitory neurons. These results parallel previous data on the function of  $\gamma\text{CaMKII}$  *in vivo* [18] and indicate that  $\gamma\text{CaMKII}$  can mediate NMDAR signaling for inducing  $\text{LTP}_{\text{E} \rightarrow \text{I}}$ .

### Activity-Dependent Translocation of $\gamma\text{CaMKII}$ in Inhibitory Interneurons

A remarkable feature of  $\gamma\text{CaMKII}$  expression is that it is highly enriched in inhibitory interneurons (e.g., parvalbumin-positive neurons), with relatively fewer excitatory neurons in the hippocampus and cortex [18]. We asked whether this cell-specific distribution pattern held true in our cultured neurons. To test this, we looked for immunocytochemical evidence for the expression of CaMKII. Noting that  $\gamma\text{CaMKII}$  was the predominant isoform that functions in cultured hippocampal neurons (Fig. 2C, D), we

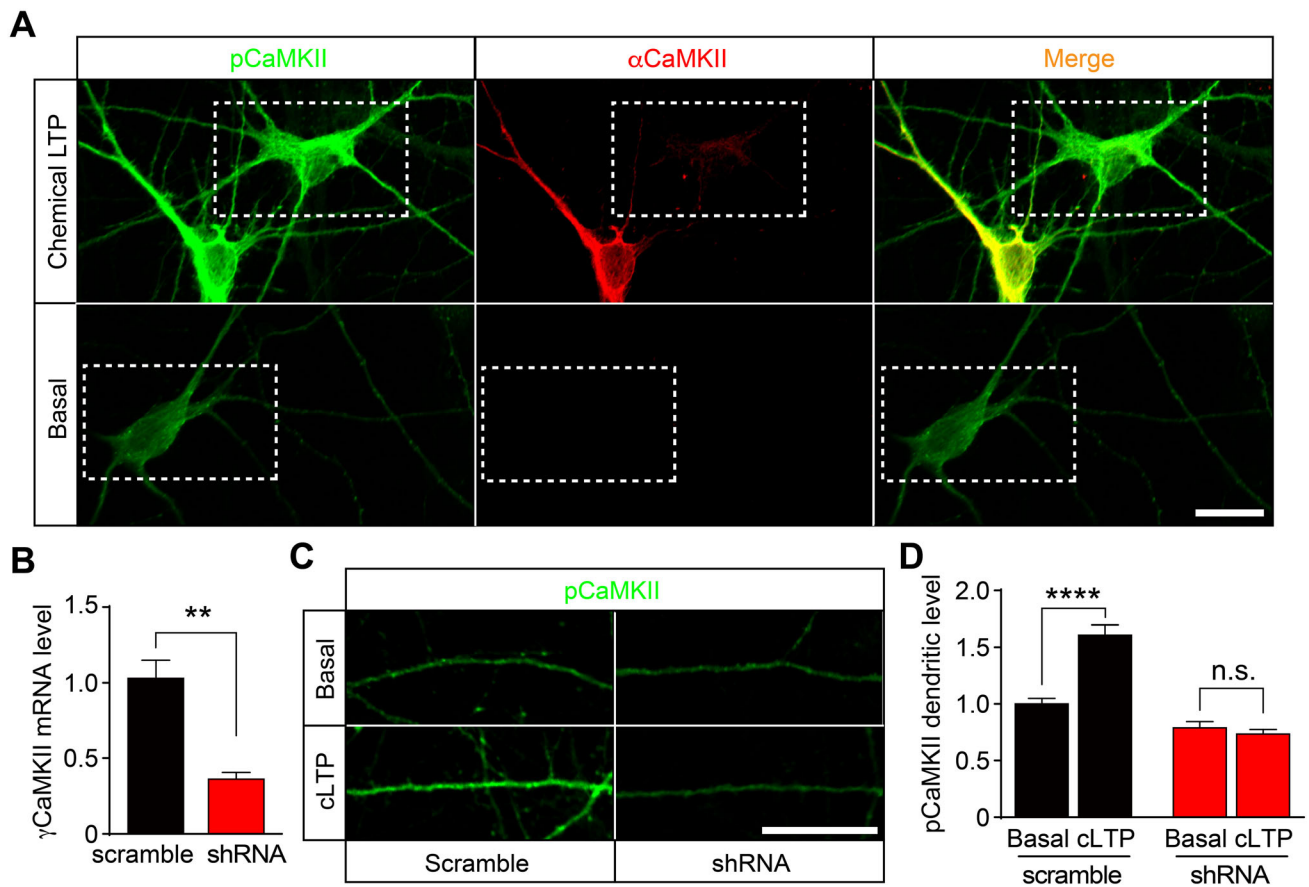


**Fig. 2**  $\gamma$ CaMKII is the major isoform of CaMKII in inhibitory interneurons. **A** Representative images of phosphorylated CaMKII (pCaMKII) in  $\alpha$ CaMKII-negative neurons under basal conditions and following cLTP stimuli. **B**  $\gamma$ CaMKII shRNA construct validated using RT-PCR.  $\gamma$ CaMKII shRNA reduces the level of endogenous  $\gamma$ CaMKII mRNA. Data are normalized to the scrambled group ( $n =$

3 batches of cells). **C**, **D** Representative images (**C**) and analysis (**D**) of dendritic pCaMKII in  $\alpha$ CaMKII-negative neurons under basal conditions and following cLTP stimuli. The cLTP-induced increase in pCaMKII is inhibited by shRNA-mediated  $\gamma$ CaMKII knockdown ( $n = 40$ – $43$  cells from two independent cultures). Unpaired Student's *t*-test,  $**P < 0.01$  and  $****P < 0.0001$ . Scale bar, 20  $\mu$ m.

monitored immunoreactivity to an anti- $\gamma$ CaMKII antibody. This antibody was specific to  $\gamma$ CaMKII as its level decreased  $\sim 75\%$  in the presence of  $\gamma$ CaMKII shRNA (Fig. 3A, B). Importantly, we found strong expression of  $\gamma$ CaMKII in  $\alpha$ CaMKII-negative neurons, which had few spines and were likely interneurons (Fig. 3C, D). Immunostaining revealed that  $\gamma$ CaMKII expression was  $>3$ -fold higher in  $\alpha$ CaMKII-negative cells than in  $\alpha$ CaMKII-positive neurons (Fig. 3C, D).

Next, we used immunogold electron microscopy to determine the subcellular localization of  $\gamma$ CaMKII. In the hippocampus, we found that  $\gamma$ CaMKII was frequently distributed near the postsynaptic density (PSD) on the dendritic shaft (Fig. 4A, B), where excitatory neurons likely form synapses with GABAergic neurons. The postsynaptic enrichment of  $\gamma$ CaMKII and its key role in  $LTP_{E \rightarrow I}$  are reminiscent of how  $\alpha$ CaMKII is recruited to the PSD where signaling *via* synaptic NMDARs regulates AMPARs and induces  $LTP_{E \rightarrow E}$  [2, 3, 12]. Given that

AMPA receptors are also the principal mediator of fast excitatory synaptic neurotransmission in interneurons [14–16], we hypothesized that  $\gamma$ CaMKII might translocate to the synapse where synaptic plasticity occurs. To test this hypothesis, we measured the subcellular localization of  $\gamma$ CaMKII with or without NMDA treatment using immunocytochemistry. We found that  $\gamma$ CaMKII was diffusely expressed in dendrites under basal conditions (Fig. 4C, D). Importantly,  $\gamma$ CaMKII was co-localized with PSD-95 (Fig. 4C, D) following NMDA stimulation, suggesting the activity-dependent recruitment of  $\gamma$ CaMKII to postsynaptic sites, where it plays an important role in synaptic plasticity. In addition, the nuclear translocation of  $\gamma$ CaMKII in excitatory neurons has been shown to be critical for excitation-transcription coupling [20, 21]. Moreover, knocking out  $\gamma$ CaMKII selectively impairs the late-phase LTP of excitatory neurons and long-term memory [21]. To test whether there is an activity-dependent nuclear translocation of  $\gamma$ CaMKII in inhibitory neurons, we

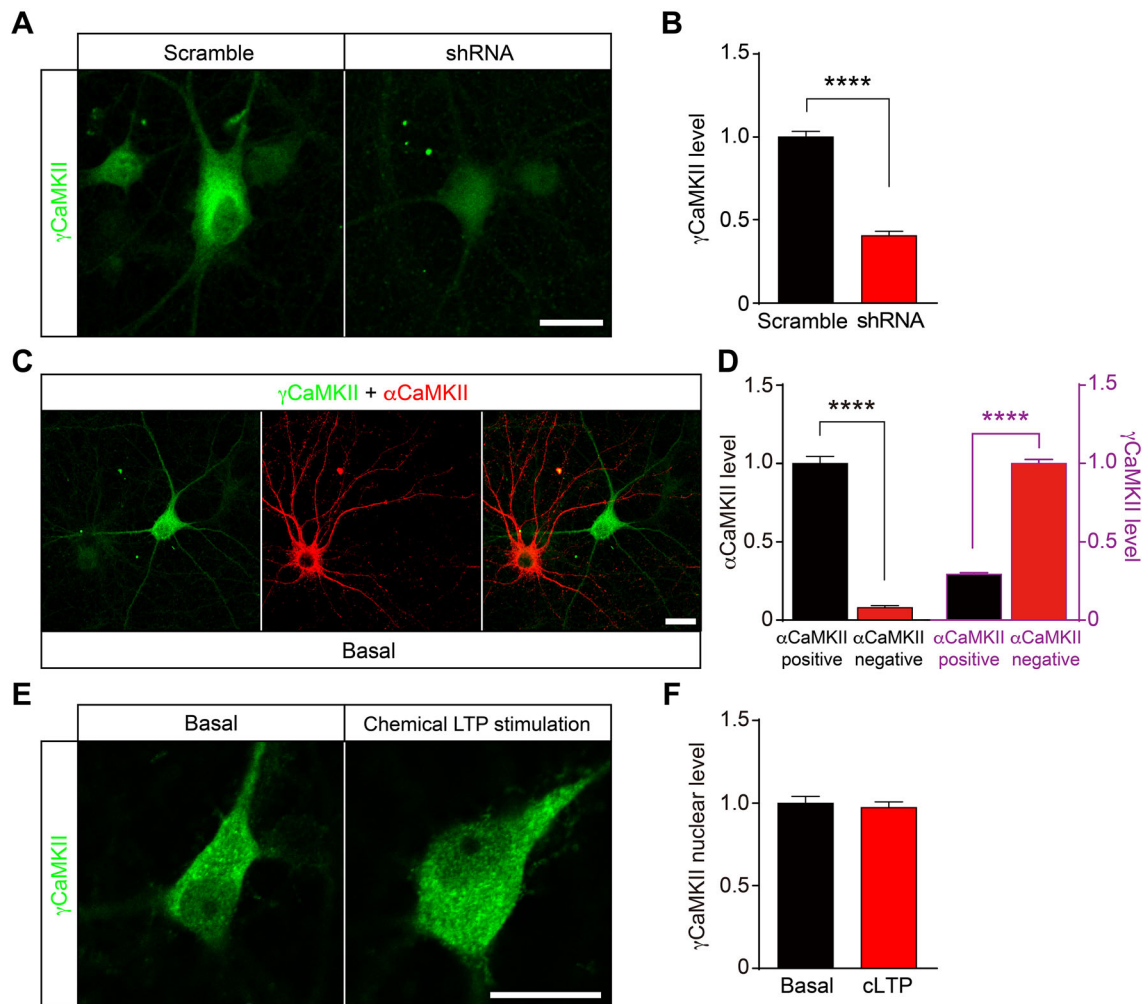


**Fig. 3** High expression of  $\gamma$ CaMKII in cultured putative inhibitory interneurons. **A, B**  $\gamma$ CaMKII shRNA construct validated using immunofluorescence. Representative images (**A**) and summary (**B**) show  $\gamma$ CaMKII shRNA knocks down the expression of  $\gamma$ CaMKII. Data are normalized to the scrambled control. **C, D** Representative image (**C**) and summary (**D**) of normalized  $\alpha$ CaMKII and  $\gamma$ CaMKII

immunoreactivity in  $\alpha$ CaMKII-positive and  $\alpha$ CaMKII-negative hippocampal neurons.  $n = 26$ – $28$  cells/group. **E, F** Representative images (**E**) and summary (**F**) of normalized nuclear  $\gamma$ CaMKII immunoreactivity in  $\alpha$ CaMKII-negative neurons under basal conditions or following chemical LTP stimuli ( $n = 20$  cells/group). \*\*\*\* $P < 0.0001$  (unpaired Student's  $t$ -test). Scale bar,  $20 \mu\text{m}$ .

measured nuclear  $\gamma$ CaMKII in  $\alpha$ CaMKII-negative neurons before and after stimulation with a standard glycine-based cLTP paradigm (Fig. 3E, F). Interestingly, we did not observe the activity-dependent nuclear translocation of  $\gamma$ CaMKII in  $\alpha$ CaMKII-negative neurons (Fig. 3E, F), consistent with the idea that  $\gamma$ CaMKI, but not  $\gamma$ CaMKII, is the synapto-nuclear shuttle for mediating excitation-transcription coupling in inhibitory interneurons [31].

### $\gamma$ CaMKII Regulates AMPAR Function in Putative Interneurons

A rapid increase of surface AMPARs induced by the chemical stimulation is widely accepted to have molecular mechanisms similar to the LTP induced by the electric stimulation [32]. Having confirmed that  $\gamma$ CaMKII is

activated in putative interneurons following cLTP/NMDA induction, we next measured the surface expression of GluA1. We found that cLTP increased the surface GluA1 level in putative inhibitory interneurons; these changes were prevented by knocking down  $\gamma$ CaMKII with shRNA (Fig. 5). To investigate this process further, we monitored the phosphorylation of the AMPAR subunit GluA1 at Ser831 (pGluA1), the key step downstream of CaMKII activation during LTP<sub>E→E</sub> induction in excitatory neurons [2, 3]. We found that the  $\gamma$ CaMKII shRNA, but not its scrambled control, inhibited cLTP-induced changes in pGluA1 (Fig. 6). Finally, the necessity of  $\gamma$ CaMKII in the cLTP of inhibitory interneurons was probed by an shRNA-resistant construct ( $\gamma$ CaMKII<sup>R</sup>). With endogenous  $\gamma$ CaMKII knocked down, “wild-type”  $\gamma$ CaMKII<sup>R</sup> fully rescued pGluA1 and the surface GluA1 level (Figs. 5, 6). In

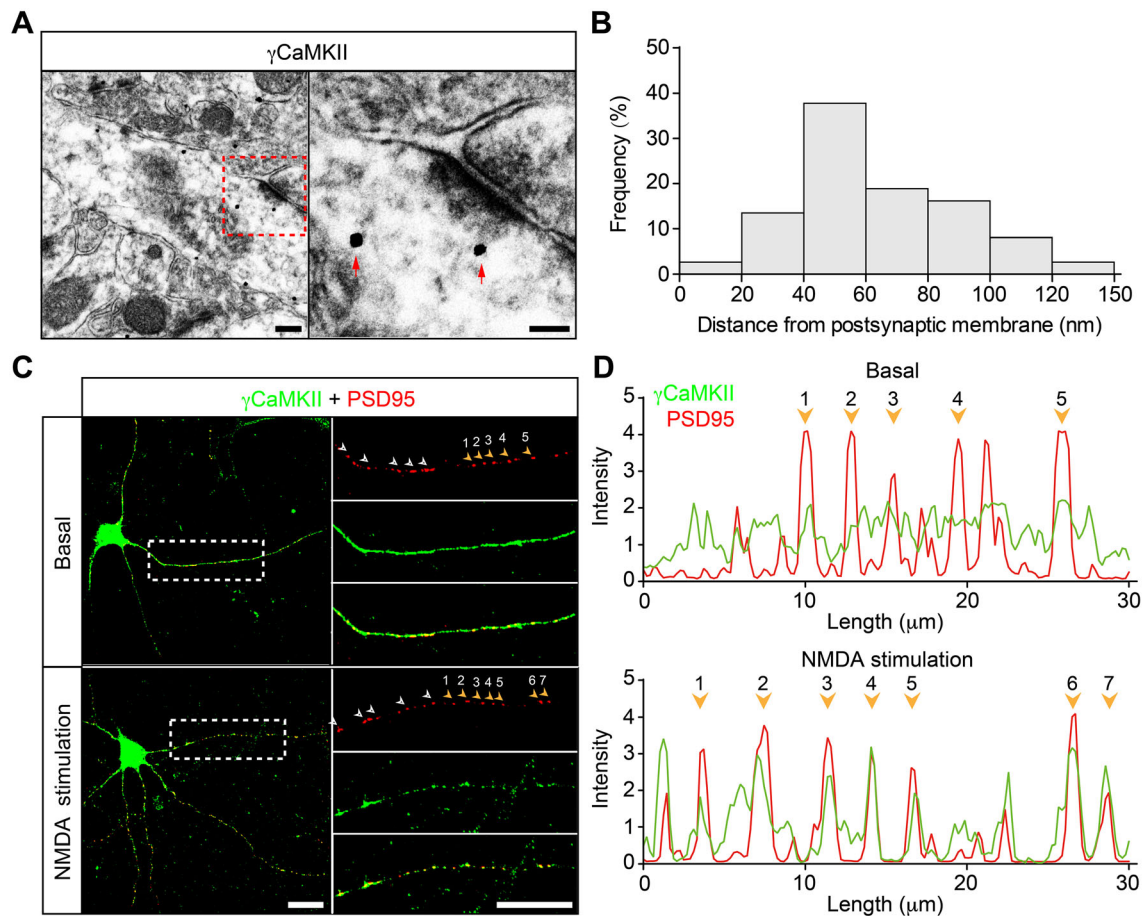


**Fig. 4** Subcellular localization and translocation of  $\gamma$ CaMKII. **A** Immuno-gold labeling of  $\gamma$ CaMKII (red arrows) in the dendritic shaft is near postsynaptic synapses. **B** Frequency distribution of distances between  $\gamma$ CaMKII-labeled gold particles and the membrane of the postsynaptic neuron. **C** Representative images of  $\gamma$ CaMKII and

the postsynaptic marker PSD-95 in cultured  $\alpha$ CaMKII-negative neurons under basal conditions (upper) or following the stimulation with 30  $\mu$ mol/L NMDA (lower). **D** Co-localization of PSD-95 and  $\gamma$ CaMKII on 30 mm-length dendrites in **(C)** (orange arrows and numbers indicate PSD-95). Scale bars, 100 nm (**A**) and 20  $\mu$ m (**C**).

contrast,  $\gamma$ CaMKII<sup>R</sup> K43R (the kinase-dead form [20]) was unable to rescue them (Figs. 5, 6), indicating that the kinase activity of  $\gamma$ CaMKII is required to regulate AMPARs during cLTP of inhibitory interneurons.

## Discussion

Although LTP<sub>E→I</sub> was reported decades ago [6], little is known about the molecular mechanism underlying this fundamental plasticity process. Recently, we found that  $\gamma$ CaMKII is the long-sought “ $\alpha$ CaMKII-like molecule” that is enriched in inhibitory interneurons and mediates LTP<sub>E→I</sub> [18]. However, how  $\gamma$ CaMKII mediates LTP<sub>E→I</sub> remained largely unclear. Here we showed that  $\gamma$ CaMKII is strongly expressed in cultured  $\alpha$ CaMKII-negative neurons and is a postsynaptic protein. Following neuronal activation,  $\gamma$ CaMKII is translocated to the synapse, where it is co-localized with PSD-95 in putative inhibitory

interneurons. Knocking down  $\gamma$ CaMKII impairs plastic changes of surface GluA1 and pGluA1 level during cLTP. Moreover, using mutated  $\gamma$ CaMKII, we found that its kinase activity is required for this process. Together, these data suggest that  $\gamma$ CaMKII is the specific CaMKII isoform that decodes NMDAR signaling and in turn regulates AMPAR function during LTP of inhibitory interneurons.

By coordinating with excitatory neurons, the plasticity of inhibitory interneurons is essential for dynamic control of the overall level of excitatory activity and information processing [6–8, 33–37]. Although CaMKII has been hypothesized to function as a mediator of LTP in inhibitory interneurons for many years [26, 27], only recently has the identity of the CaMKII isoform— $\gamma$ CaMKII—been uncovered [18]. The expression of the AMPAR subunits in inhibitory interneurons is similar to that in excitatory neurons; they can express either GluA2-lacking, Ca<sup>2+</sup>-permeable AMPARs or GluA2-containing, Ca<sup>2+</sup>-impermeable AMPARs [16]. Interestingly, in synapses



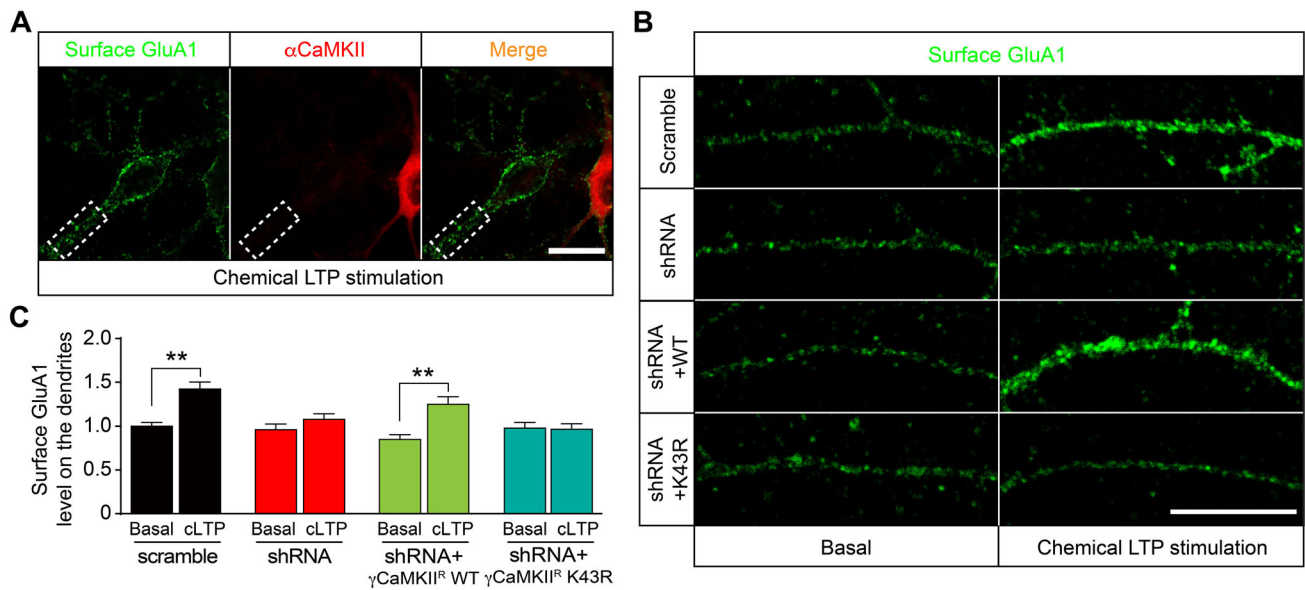


**Fig. 5**  $\gamma$ CaMKII regulates AMPAR trafficking in cultured interneurons. **A–C** Representative images (**A**, **B**) and analysis (**C**) of dendritic surface GluA1 measured in cultured putative interneurons under basal conditions and following cLTP stimuli; where indicated, cells express scrambled control shRNA,  $\gamma$ CaMKII shRNA, or  $\gamma$ CaMKII shRNA

together with either shRNA-resistant wild-type  $\gamma$ CaMKII ( $\gamma$ CaMKII<sup>R</sup>) or an shRNA-resistant kinase-disabled mutant form of  $\gamma$ CaMKII ( $\gamma$ CaMKII<sup>R</sup> K43R) ( $n = 19$ – $50$  cells from two independent cultures).  $**P < 0.01$  (one-way ANOVA followed by Tukey's test). Scale bar, 20  $\mu$ m.

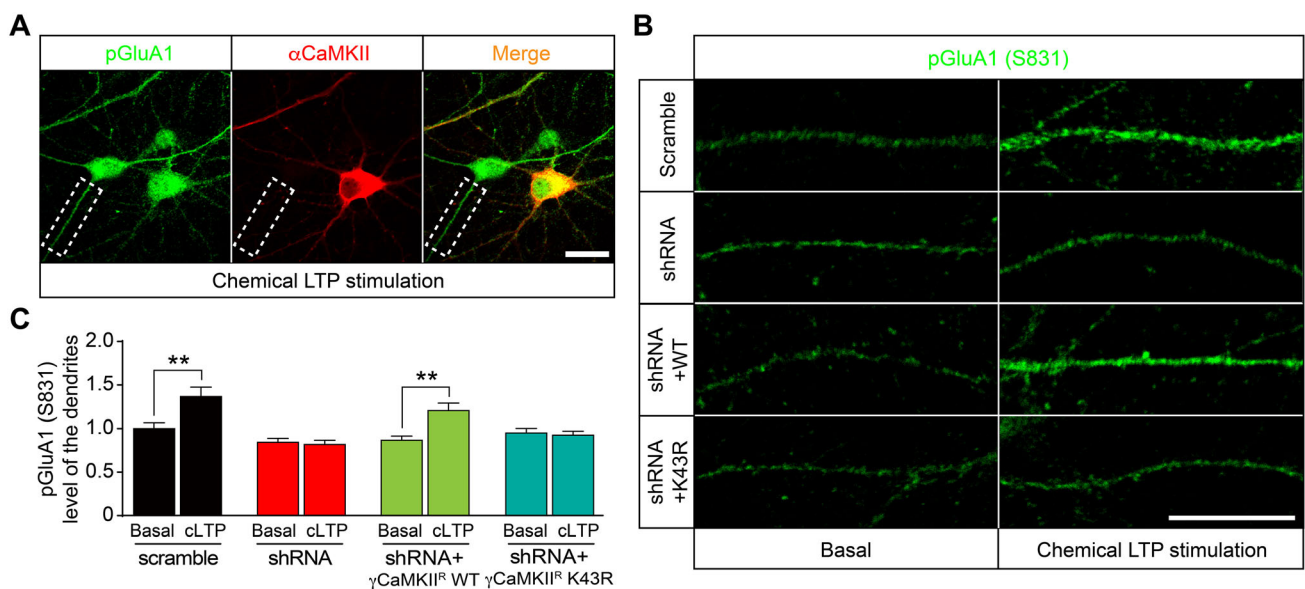


**Fig. 6**  $\gamma$ CaMKII regulates AMPAR phosphorylation in cultured interneurons. **A–C** Representative images (**A**, **B**) and summary data (**C**) of dendritic phosphorylated GluA1 measured in cultured putative interneurons under basal conditions and following cLTP stimulation; where indicated, cells express scrambled control shRNA,  $\gamma$ CaMKII

shRNA, or  $\gamma$ CaMKII shRNA together with either shRNA-resistant wild-type  $\gamma$ CaMKII ( $\gamma$ CaMKII<sup>R</sup>) or an shRNA-resistant kinase-dead mutant form of  $\gamma$ CaMKII ( $\gamma$ CaMKII<sup>R</sup> K43R) ( $n = 39$ – $43$  cells from two independent cultures).  $**P < 0.01$  (one-way ANOVA followed by Tukey's test). Scale bar, 20  $\mu$ m.

comprising GluA2-containing AMPARs that are localized on interneurons derived from the medial ganglionic eminence of the ventral telencephalon, the GluN2A-containing NMDAR currents are typically small [16, 19]. As the activation of  $\alpha$ CaMKII in excitatory neurons requires NMDAR-mediated signaling [2, 3, 5, 12], it is

logical to ask whether  $\gamma$ CaMKII can still decode synaptic information if NMDAR-mediated currents are relatively small. In this regard, our finding that  $\gamma$ CaMKII is recruited by cLTP stimulation and controls AMPAR functions provides a piece of evidence supporting the hypothesis that  $\gamma$ CaMKII is the mediator of NMDAR-dependent LTP

in inhibitory interneurons. Collectively, these results are consistent with the idea that a local increase of  $\text{Ca}^{2+}$  near NMDAR and L-type  $\text{Ca}^{2+}$  channels [38] can activate CaMKII when voltage-gated conformational changes of these channels are induced by neuronal stimuli.

The molecular pathway that leads to the long-lasting plasticity of glutamatergic transmission has been extensively studied in excitatory synapses onto excitatory neurons ( $\text{LTP}_{\text{E} \rightarrow \text{E}}$ ) [2–5, 39]. Activated by postsynaptic NMDAR  $\text{Ca}^{2+}$  signaling [40],  $\alpha$ CaMKII is necessary and sufficient to generate  $\text{LTP}_{\text{E} \rightarrow \text{E}}$  by regulating AMPAR function [2, 3, 5, 12]. However, it remains unclear whether the finding about the molecular mechanism underlying LTP in excitatory neurons can be generalized to that in inhibitory interneurons, given that interneurons are known to have high structural and functional diversity [34, 36]. For example, as a major subtype of inhibitory interneurons, parvalbumin-positive ( $\text{PV}^+$ ) interneurons are remarkable for their fast-spiking phenotype, firing action potentials much faster than excitatory neurons [41, 42]. The intense activity of  $\text{PV}^+$  interneurons might cause larger and longer elevations of  $\text{Ca}^{2+}$  that could potentially saturate a replica of the machinery described in excitatory neurons [31]. In line with this, we found that  $\gamma$ CaMKII in putative interneurons is preferentially activated by high-frequency stimuli. Indeed, the enriched  $\gamma$ CaMKII in inhibitory interneurons could enjoy a functional advantage over other CaMKII subunits, as  $\gamma$ CaMKII has the slowest autophosphorylation rate [29], which makes it ideally suited for decoding the  $\text{Ca}^{2+}$  signals (often long-lasting) in  $\text{PV}^+$  interneurons [31]. Interestingly, several studies have found an association between both  $\gamma$ CaMKII [43–46] and inhibitory interneurons [37, 47–49], and a variety of neuropsychiatric disorders, including Alzheimer's disease, autism, and schizophrenia [50, 51], suggesting that signaling pathways implicated in LTP of inhibitory interneurons may be implicated in these disorders.

**Acknowledgements** We thank Yulong Li for providing the equipment for the field stimulation. We also thank Chengfeng Ye for careful reading of the manuscript. This work was supported by Science and Technology Innovation 2030-Major Project (2021ZD0203501), the National Natural Science Foundation of China (81930030, 31771109, and 31722023); the National Key R&D Program of China (2019YFA0508603); CAMS Innovation Fund for Medical Sciences (2019-I2M-5-057); Project for Hangzhou Medical Disciplines of Excellence; Key Project for Hangzhou Medical Disciplines; the Fundamental Research Funds for the Central Universities of China (2018XZZX002-02, 2019XZZX001-01-04, and 2019FZA7009); and the National Postdoctoral Program for Innovative Talents (BX2021263).

**Conflict of interest** The authors claim that there are no conflicts of interest.

## References

- Bliss TV, Collingridge GL. A synaptic model of memory: Long-term potentiation in the hippocampus. *Nature* 1993, 361: 31–39.
- Malenka RC, Nicoll RA. Long-term potentiation—a decade of progress? *Science* 1999, 285: 1870–1874.
- Malinow R, Mainen ZF, Hayashi Y. LTP mechanisms: From silence to four-lane traffic. *Curr Opin Neurobiol* 2000, 10: 352–357.
- Mayford M, Siegelbaum SA, Kandel ER. Synapses and memory storage. *Cold Spring Harb Perspect Biol* 2012, 4: a005751.
- Silva AJ, Stevens CF, Tonegawa S, Wang Y. Deficient hippocampal long-term potentiation in alpha-calcium-calmodulin kinase II mutant mice. *Science* 1992, 257: 201–206.
- Buzsáki G, Eidelberg E. Direct afferent excitation and long-term potentiation of hippocampal interneurons. *J Neurophysiol* 1982, 48: 597–607.
- Kullmann DM, Moreau AW, Bakiri Y, Nicholson E. Plasticity of inhibition. *Neuron* 2012, 75: 951–962.
- Pelkey KA, Chittajallu R, Craig MT, Tricoire L, Wester JC, McBain CJ. Hippocampal GABAergic inhibitory interneurons. *Physiol Rev* 2017, 97: 1619–1747.
- Pelletier JG, Lacaille JC. Long-term synaptic plasticity in hippocampal feedback inhibitory networks. *Prog Brain Res* 2008, 169: 241–250.
- Morris RG, Anderson E, Lynch GS, Baudry M. Selective impairment of learning and blockade of long-term potentiation by an N-methyl-D-aspartate receptor antagonist, AP5. *Nature* 1986, 319: 774–776.
- Herring BE, Nicoll RA. Long-term potentiation: From CaMKII to AMPA receptor trafficking. *Annu Rev Physiol* 2016, 78: 351–365.
- Hell JW. CaMKII: claiming center stage in postsynaptic function and organization. *Neuron* 2014, 81: 249–265.
- Lisman J, Schulman H, Cline H. The molecular basis of CaMKII function in synaptic and behavioural memory. *Nat Rev Neurosci* 2002, 3: 175–190.
- Allen K, Monyer H. Interneuron control of hippocampal oscillations. *Curr Opin Neurobiol* 2015, 31: 81–87.
- Bartos M, Vida I, Jonas P. Synaptic mechanisms of synchronized gamma oscillations in inhibitory interneuron networks. *Nat Rev Neurosci* 2007, 8: 45–56.
- Akgül G, McBain CJ. Diverse roles for ionotropic glutamate receptors on inhibitory interneurons in developing and adult brain. *J Physiol* 2016, 594: 5471–5490.
- Liu XB, Jones EG. Localization of alpha type II calcium calmodulin-dependent protein kinase at glutamatergic but not gamma-aminobutyric acid (GABAergic) synapses in thalamus and cerebral cortex. *Proc Natl Acad Sci U S A* 1996, 93: 7332–7336.
- He XZ, Li JR, Zhou GJ, Yang J, McKenzie S, Li YJ. Gating of hippocampal rhythms and memory by synaptic plasticity in inhibitory interneurons. *Neuron* 2021, 109: 1013–1028.e9.
- Matta JA, Pelkey KA, Craig MT, Chittajallu R, Jeffries BW, McBain CJ. Developmental origin dictates interneuron AMPA and NMDA receptor subunit composition and plasticity. *Nat Neurosci* 2013, 16: 1032–1041.
- Ma H, Groth RD, Cohen SM, Emery JF, Li BX, Hoedt E, *et al.*  $\gamma$ CaMKII shuttles  $\text{Ca}^{2+}$ /CaM to the nucleus to trigger CREB phosphorylation and gene expression. *Cell* 2014, 159: 281–294.
- Cohen SM, Suutari B, He XZ, Wang Y, Sanchez S, Tirko NN, *et al.* Calmodulin shuttling mediates cytonuclear signaling to trigger experience-dependent transcription and memory. *Nat Commun* 2018, 9: 2451.

22. Hudmon A, Schulman H. Neuronal Ca<sup>2+</sup>/calmodulin-dependent protein kinase II: The role of structure and autoregulation in cellular function. *Annu Rev Biochem* 2002, 71: 473–510.
23. de Koninck P, Schulman H. Sensitivity of CaM kinase II to the frequency of Ca<sup>2+</sup> oscillations. *Science* 1998, 279: 227–230.
24. Fujii H, Inoue M, Okuno H, Sano Y, Takemoto-Kimura S, Kitamura K, *et al.* Nonlinear decoding and asymmetric representation of neuronal input information by CaMKII $\alpha$  and calcineurin. *Cell Rep* 2013, 3: 978–987.
25. Wheeler DG, Groth RD, Ma H, Barrett CF, Owen SF, Safa P, *et al.* Ca<sub>v1</sub> and Ca<sub>v2</sub> channels engage distinct modes of Ca<sup>2+</sup> signaling to control CREB-dependent gene expression. *Cell* 2012, 149: 1112–1124.
26. Wang JH, Kelly P. Calcium-calmodulin signalling pathway up-regulates glutamatergic synaptic function in non-pyramidal, fast spiking rat hippocampal CA1 neurons. *J Physiol* 2001, 533: 407–422.
27. Lamsa K, Irvine EE, Giese KP, Kullmann DM. NMDA receptor-dependent long-term potentiation in mouse hippocampal interneurons shows a unique dependence on Ca<sup>2+</sup>/calmodulin-dependent kinases. *J Physiol* 2007, 584: 885–894.
28. Pan Y, He XZ, Li CC, Li YJ, Li WW, Zhang HB, *et al.* Neuronal activity recruits the CRTCI/CREB axis to drive transcription-dependent autophagy for maintaining late-phase LTD. *Cell Rep* 2021, 36: 109398.
29. Gaertner TR, Kolodziej SJ, Wang D, Kobayashi R, Koomen JM, Stoops JK, *et al.* Comparative analyses of the three-dimensional structures and enzymatic properties of alpha, beta, gamma and delta isoforms of Ca<sup>2+</sup>-calmodulin-dependent protein kinase II. *J Biol Chem* 2004, 279: 12484–12494.
30. Bayer KU, de Koninck P, Schulman H. Alternative splicing modulates the frequency-dependent response of CaMKII to Ca<sup>2+</sup> oscillations. *EMBO J* 2002, 21: 3590–3597.
31. Cohen SM, Ma H, Kuchibhotla KV, Watson BO, Buzsáki G, Froemke RC, *et al.* Excitation-transcription coupling in parvalbumin-positive interneurons employs a novel CaM kinase-dependent pathway distinct from excitatory neurons. *Neuron* 2016, 90: 292–307.
32. Lu W, Man H, Ju W, Trimble WS, MacDonald JF, Wang YT. Activation of synaptic NMDA receptors induces membrane insertion of new AMPA receptors and LTP in cultured hippocampal neurons. *Neuron* 2001, 29: 243–254.
33. Froemke RC. Plasticity of cortical excitatory-inhibitory balance. *Annu Rev Neurosci* 2015, 38: 195–219.
34. Kepecs A, Fishell G. Interneuron cell types are fit to function. *Nature* 2014, 505: 318–326.
35. Isaacson JS, Scanziani M. How inhibition shapes cortical activity. *Neuron* 2011, 72: 231–243.
36. Klausberger T, Somogyi P. Neuronal diversity and temporal dynamics: The unity of hippocampal circuit operations. *Science* 2008, 321: 53–57.
37. Hu H, Gan J, Jonas P. Interneurons. Fast-spiking, parvalbumin<sup>+</sup> GABAergic interneurons: From cellular design to microcircuit function. *Science* 2014, 345: 1255263.
38. Li BX, Tadross MR, Tsien RW. Sequential ionic and conformational signaling by calcium channels drives neuronal gene expression. *Science* 2016, 351: 863–867.
39. Lisman J, Yasuda R, Raghavachari S. Mechanisms of CaMKII action in long-term potentiation. *Nat Rev Neurosci* 2012, 13: 169–182.
40. Tsien JZ, Huerta PT, Tonegawa S. The essential role of hippocampal CA1 NMDA receptor-dependent synaptic plasticity in spatial memory. *Cell* 1996, 87: 1327–1338.
41. Kawaguchi Y, Hama K. Fast-spiking non-pyramidal cells in the hippocampal CA3 region, dentate gyrus and subiculum of rats. *Brain Res* 1987, 425: 351–355.
42. Royer S, Zemelman BV, Losonczy A, Kim J, Chance F, Magee JC, *et al.* Control of timing, rate and bursts of hippocampal place cells by dendritic and somatic inhibition. *Nat Neurosci* 2012, 15: 769–775.
43. de Ligt J, Willemsen MH, van Bon BWM, Kleefstra T, Yntema HG, Kroes T, *et al.* Diagnostic exome sequencing in persons with severe intellectual disability. *N Engl J Med* 2012, 367: 1921–1929.
44. Peixoto LL, Wimmer ME, Poplawski SG, Tudor JC, Kenworthy CA, Liu SC, *et al.* Memory acquisition and retrieval impact different epigenetic processes that regulate gene expression. *BMC Genomics* 2015, 16(Suppl 5): S5.
45. Voineagu I, Wang XC, Johnston P, Lowe JK, Tian Y, Horvath S, *et al.* Transcriptomic analysis of autistic brain reveals convergent molecular pathology. *Nature* 2011, 474: 380–384.
46. de Quervain DJF, Papassotiropoulos A. Identification of a genetic cluster influencing memory performance and hippocampal activity in humans. *Proc Natl Acad Sci U S A* 2006, 103: 4270–4274.
47. Marín O. Interneuron dysfunction in psychiatric disorders. *Nat Rev Neurosci* 2012, 13: 107–120.
48. Gillespie AK, Jones EA, Lin YH, Karlsson MP, Kay K, Yoon SY, *et al.* Apolipoprotein E4 causes age-dependent disruption of slow gamma oscillations during hippocampal sharp-wave ripples. *Neuron* 2016, 90: 740–751.
49. Verret L, Mann EO, Hang GB, Barth AM, Cobos I, Ho K, *et al.* Inhibitory interneuron deficit links altered network activity and cognitive dysfunction in Alzheimer model. *Cell* 2012, 149: 708–721.
50. Liu YQ, Yu F, Liu WH, He XH, Peng BW. Dysfunction of hippocampal interneurons in epilepsy. *Neurosci Bull* 2014, 30: 985–998.
51. Wu QQ, Wang XY, Wang Y, Long YJ, Zhao JP, Wu RR. Developments in biological mechanisms and treatments for negative symptoms and cognitive dysfunction of schizophrenia. *Neurosci Bull* 2021, 37: 1609–1624.